3. Sinusas AJ, Trautman KA, Bergin JD, et al. Quantification of area at risk during coronary occlusion and degree of myocardial salvage after reperfusion with technetium-99m-methoxyisobutyl-isonitrile. *Circulation* 1990;82:1424–1437.
4. Medrano R, Weilbaacher D, Young JB, et al. Assessment of myocardial viability with technetium-99m sestamibi in patients undergoing cardiac transplantation: a scintigraphic-pathologic study [Abstract]. *Circulation* 1992;86(suppl I):I-108.
5. Gibbons RJ, Verani MS, Behrenbeck T, et al. Feasibility of tomographic ^{99m}Tc-hexakis-2 methoxy-2 methylpropyl-isonitrile imaging for the assessment of myocardial area at risk and the effect of treatment in acute myocardial infarction. *Circulation* 1989;80:1277–1286.
6. O'Connor MK, Hammell TC, Gibbons RJ. In vitro validation of a simple tomographic technique for estimation of percent myocardium at risk following administration of Tc99m isonitrile. *Eur J Nucl Med* 1990;17:69–76.
7. Maron BJ, Henry WL, Roberts WC, et al. Comparison of echocardiographic and necropsy measurements of ventricular wall thicknesses in patients with and without disproportionate septal thickening. *Circulation* 1977;55:341–346.
8. Edwards WD. Pathology of myocardial infarction and reperfusion. In: Gersh BJ, Rahimtoola SH, eds. *Acute myocardial infarction*. New York: Elsevior; 1991:14–48.
9. Lowe JE, Reimer KA, Jennings RB. Experimental infarct size as a function of the amount of myocardium at risk. *Am J Pathol* 1978;90:373–376.
10. Reimer KA, Jennings RB, Cobb RF, et al. Animal models for protecting ischemic myocardium: results of the NHLBI Cooperative Study. Comparison of unconscious and conscious dog models. *Circ Res* 1985;56:651–665.
11. Miller TD, Christian TF, Hopfenspirger MR, Hodge DO, Gersh BJ, Gibbons RJ. Infarct size after acute myocardial infarction measured by quantitative tomographic ^{99m}Tc sestamibi imaging predicts subsequent mortality. *Circulation* 1995;92:334–341.
12. Feiring AJ, Johnson MR, Kioschos JM, Kirchner PT, Marcus ML, White CW. The importance of the determination of the myocardial area at risk in the evaluation of the outcome of acute myocardial infarction in patients. *Circulation* 1987;75:980–987.
13. Gibbons RJ, Christian TF, Hopfenspirger M, Hodge DO, Bailey KR. Myocardium at risk and infarct size after thrombolytic therapy for acute myocardial infarction: implications for the design of randomized trials of acute intervention. *J Am Coll Cardiol* 1994;24:616–623.

Technetium-99m MIBI to Assess Coronary Collateral Flow During Acute Myocardial Infarction in Two Closed-Chest Animal Models

Timothy F. Christian, Michael K. O'Connor, Robert S. Schwartz, Raymond J. Gibbons and Erik L. Ritman
Division of Cardiovascular Diseases and Internal Medicine and Departments of Nuclear Medicine and Physiology, Mayo Clinic and Mayo Foundation, Rochester, Minnesota

Collateral flow is an independent determinant of infarct size in both animal and clinical studies of myocardial infarction. The purpose of this study was to quantitatively evaluate, in a closed-chest animal model, a noninvasive method of measuring coronary collateral flow over a wide spectrum of collateral flow rates from a tracer that can be injected during occlusion but measured after reperfusion. **Methods:** Fourteen animals underwent 40 min of coronary occlusion using a closed-chest technique. Two closed-chest models representing different rates of collateral flow were used: canine and porcine. Coronary blood flow was measured by radiolabeled microspheres. Collateral blood within the risk zone was estimated from the severity of ^{99m}Tc-sestamibi tomographic perfusion defect. **Results:** Collateral blood flow was significantly higher in the canine model than it was in the porcine model. There was close agreement ($r = 0.90$) between absolute collateral flow by microspheres and the severity of the tomographic perfusion defect. **Conclusion:** These results suggest that an accurate noninvasive estimate of collateral blood flow can be provided by an intravenous injection of ^{99m}Tc-sestamibi.

Key Words: collateral circulation; radionuclide imaging; coronary blood flow

J Nucl Med 1997; 38:1840–1846

Collateral flow to jeopardized myocardium is an important determinant of outcome during acute myocardial infarction. Animal studies of reperfusion have established the magnitude of collateral flow as one of the four independent determinants of infarct size (in addition to the extent of the risk area, metabolic demand and duration of occlusion) (*1,2*) and as the primary factor in extending the window of time for which late coronary reperfusion can be of benefit (*2*). The importance of collateral flow as a determinant of infarct size has been confirmed in clinical studies (*3–5*). However, assessment of collateral flow in patients during acute myocardial infarction is still a problem. Angiographic assessment of collaterals is strongly associated with subsequent outcome during myocardial infarction but is not always available or feasible before thrombolytic therapy (*3–6*). Invasive contrast echocardiography has been used in the weeks after infarction to assess collateral flow but has not been used clinically with an intravenous injection during acute myocardial infarction (*7*).

In a previous clinical study, we described the use of the severity of the perfusion defect by tomographic perfusion imaging after the intravenous injection with ^{99m}Tc-sestamibi to assess collateral flow during the acute stages of myocardial infarction (*4*). This measurement was strongly associated with the presence of angiographic collaterals before reperfusion therapy and was a significant determinant of final infarct size, which was independent of myocardium at risk and time to reperfusion. The purpose of this study was to validate a noninvasive tomographic imaging method for the assessment of collateral flow, which can be initiated during coronary artery occlusion but acquired after reperfusion by comparing its performance to true myocardial blood flow during occlusion, determined by radiolabeled microspheres in closed-chest animal models. This replicates the clinical situation for which this technique has been used (*4*). To test this measure over a range of collateral flows, two models were used: a canine model, in which native collateral flow is expected to be high; and a porcine model, in which native collateral flow is expected to be low.

MATERIALS AND METHODS

Experimental Preparation Methods

Two models were used in this study. Seven mongrel dogs (weight 27 ± 2 kg; range 24 kg–29 kg) and eight pigs (weight 38 ± 5 kg; range 32 kg–45 kg) underwent general anesthesia with intravenous pentobarbitol, fentanyl and droperidol (dogs) or ketamine and fentanyl (pigs), for the canine and porcine models,

Received Aug. 13, 1996; revision accepted Feb. 24, 1997.
For correspondence or reprints contact: Timothy F. Christian, MD, Mayo Clinic, 200 First Street Southwest, East 16B, Rochester, MN 55905.

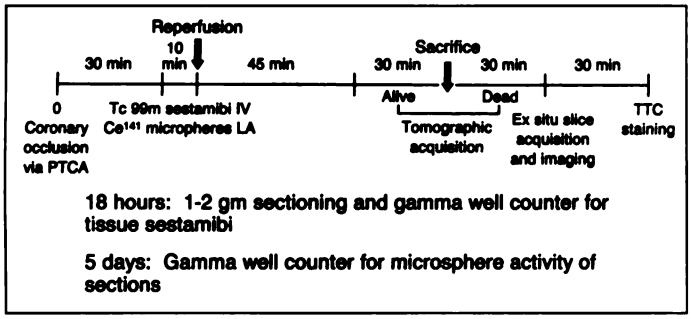

FIGURE 1. Experimental protocol for the two models during coronary occlusion using a balloon catheter.

respectively. The animals were intubated and mechanically ventilated with supplemental oxygen (40% $Fi0_2$) for both models. Five catheters were introduced percutaneously into each animal with fluoroscopic guidance: a cardiac pacing catheter into the coronary sinus, an intravenous catheter, a catheter into the descending aorta (for reference blood sampling), either a trans-septal left atrial catheter (dogs) or a left ventricular pigtail catheter (pigs) for microsphere injection and a coronary artery guide catheter for introduction of a balloon angioplasty catheter (3.0 balloon size). The angioplasty catheter was localized by fluoroscopy and contrast injection. At no time was the chest cavity opened.

Experimental Protocol

The protocol used is schematically illustrated in Figure 1. All animals were given an intravenous bolus of lidocaine (100 mg) and maintained on an intravenous lidocaine infusion of 1 mg/min. At time zero for both models, the left anterior descending artery was occluded using a 3.0-mm balloon angioplasty catheter. Systemic arterial pressure and the surface electrocardiogram were monitored before, during and after balloon occlusion. Total coronary artery occlusion was confirmed by contrast injection through the guide catheter and distal coronary artery pressure monitoring, and the electrocardiogram was monitored for ST segment elevation to confirm the presence of ischemia. After 30 min of occlusion, 25–30 mCi of ^{99m}Tc-sestamibi were injected intravenously, and 2×10^6 ^{141}Ce-labeled microspheres (50 μCi) suspended in Tween 80 (diameter = 15.5 μm) were injected into the left atrium (dogs) or left ventricular apex (pigs) simultaneously. Reference blood sampling in the descending aorta was obtained at a rate of 7.64 ml/min. After a total of 40 min of coronary occlusion, the balloon was deflated.

Imaging Protocol

Animals were placed in a triple-headed gamma camera (Triad-SS, Trionix, Inc., Twinsberg, OH) with a special cradle to enhance the reproducibility of positioning, such that the animal was suspended in the anterior supine position. Two separate tomographic scans were obtained for each animal using low-energy, medium-resolution collimators. An in vivo scan was acquired over a 360° orbit, with 40 images per head at 3° intervals, for a total of 120 views. The acquisition time per view was 20 sec, for a total imaging time of 13.3 min. The counts acquired for study were high (mean 20.0 M ± 5.7 M counts; range 12.6 M–27.8 M counts). After completion of this scan, a lethal dose of pentobarbital was administered, and in situ tomographic imaging was repeated using the same format. The heart was then excised and manually sectioned into five short-axis slices of approximately equal thickness (1 cm). These slices were then placed on the collimated camera face and imaged directly for 5 min.

Tomographic Reconstruction and Quantification

Images were processed using the same methodology used in prior clinical studies (*4,8*). These techniques have been previously described (*9*). Briefly, 1-pixel-thick transaxial slices were generated by filtered backprojection using a Ramp Hanning filter. Horizontal and vertical short-axis slices were generated from the transaxial slices. The limits of the myocardium were visually determined, and the short-axis slices were generated between these limits (*9*). Attenuation and scatter correction algorithms were not used.

Circumferential count profiles were generated for each of five representative short-axis slices (apical, midventricular, basal with intermediate slices between the apex, midventricle and base) using previously described techniques (*4,9,10*). Perfusion defect size (extent) was quantified as the number of radii (60 maximum, each at 6° intervals) with less than 60% of maximal counts per slice over the five slices and was weighted by the radius of the cavity and apical location (*4,9*). Because of the absent chest wall and anticipated reduced scatter and attenuation during the ex situ acquisition, a 50% threshold was initially used to quantify defect size for that set of images. However, there was no significant difference in defect size using a 60% or 50% threshold due to the sharp borders and severity of the defect. Consequently, for consistency, a 60% threshold was used to quantify all images.

Perfusion defect severity was calculated for each tomographic or ex situ slice using the ratio of minimum-to-maximum counts from the circumferential count profile curve (*4*). The lowest of these values from the five short-axis slices was termed the nadir and used as the single value representing collateral flow for that animal. This method exactly reproduces the noninvasive assessment of collateral flow used in clinical studies (*4*) and is independent of the threshold method of perfusion defect quantification.

Pathologic Analysis

The five ex situ short-axis slices were stained with 1% 2,3-triphenyl tetrazolium chloride (TTC) within 1 hr–1.5 hr of animal sacrifice and were subsequently photographed. The 8-in. × 10-in. photographs were digitized using an image scanner, and infarct size area was planimetered and measured using a software package (NIH Image 1.58; National Institutes of Health, Bethesda, MD). Infarct size was expressed as the ratio of infarcted myocardium-to-noninfarcted myocardium × 100 [percentage of the left ventricle (LV)], adjusted for the weight of each slice. Short-axis slices were then radially sectioned into equally sized transmural segments and placed in a gamma well counter for 5 min each to determine ^{99m}Tc-sestamibi activity at 18 hr and ^{141}Ce microsphere activity 5 days later. The number of segments per slice varied with the radius of the slice (minimum of four for the apical slice and maximum of 16 for basal slices).

Myocardial blood flow was determined for each segment from the tissue activity at 5 days and for the reference blood flow sample using a conventional formula (*11,12*). Coronary blood flow measurements were expressed as absolute measures in $ml \cdot g^{-1} min^{-1}$. Collateral flow within the center of the ischemic zone was determined by two methods to control for random fluctuations in sampling. In the first method, the lowest value of myocardial blood flow in the risk region was chosen (minimal blood flow). In the second method, a value was calculated from the average of the lowest value and the two contiguous segments adjacent to it (central ischemic blood flow). Technetium-99m-sestamibi activity was expressed as $counts \cdot min^{-1} g^{-1}$ of myocardium and also as a percentage of peak activity (normalized values). As a secondary analysis, microsphere derived blood flow was expressed as a percentage of peak flow in the heart to facilitate comparisons between animals.

Statistical Analysis

Data are expressed as mean ± s.d. Simple linear regression analysis was used to compare continuous variables, such as

perfusion defect severity, with microsphere-derived collateral blood flow. Unpaired Student t-tests were used to compare model differences, such as blood flow, sestamibi activity and infarct size between models. The primary analysis was the comparison of absolute collateral blood flow with the tomographic in vivo nadir by linear regression analysis. This was chosen because it provides a close reflection of blood flow to the tissue during occlusion. It is conceivable that normalized values to peak flow may be less reflective of actual blood flow within the ischemic zone if peak flow outside the risk area is unusually high or low. A secondary analysis was the comparison of normalized collateral blood flow values with the tomographic in vivo nadir. All analyses were performed using commercially available software.

RESULTS

A total of 15 animals were included in the study: 7 dogs in the closed-chest canine model and 8 pigs in the closed-chest porcine model. One animal (canine) died before acquisition of the perfusion images and was subsequently excluded from the study, leaving six animals in the canine group for analysis.

Hemodynamics

There were significant hemodynamic changes that occurred during the 40-min coronary occlusion, although the response did not differ by model. Heart rate significantly increased from baseline (101 ± 16 bpm preocclusion compared to 126 ± 35 bpm during coronary occlusion; $p < 0.05$). Mean systemic arterial blood pressure significantly fell from basal measurements (89 ± 10 mmHg preocclusion compared to 79 ± 12 mm Hg during occlusion; $p < 0.05$). Total coronary artery occlusion using the balloon angioplasty catheter was confirmed in all animals by contrast injection through a left coronary guide catheter and distal coronary artery pressure monitoring.

Tissue Analysis

There was an excellent linear correlation between ^{99m}Tc-sestamibi uptake and the degree of myocardial blood flow measured by radiolabeled microspheres during coronary occlusion for both models, despite the presence of prolonged reperfusion flow (1.5 hr–2.0 hr), both in regions with reduced flow and nonischemic regions. Normalized measures are shown in Figure 2. The correlation coefficients for non-normalized measurements for individual animals on a segment by segment basis in the canine model ranged from $r = 0.89$ to $r = 0.98$, with a median r value from the six animals of $r = 0.94$. Correlation coefficients for the porcine model were equally good, ranging from $r = 0.88$ to $r = 1.0$, with a median correlation coefficient of $r = 0.98$ for the eight animals in this model. Consequently, there was good concordance on a tissue level between flow and isotope uptake. There was a small but consistent overestimation of flow by sestamibi uptake, however, that was more pronounced in the canine model (Fig. 2).

Risk Area and Infarct Size

The risk area calculated from the ^{99m}Tc-sestamibi ex situ slice perfusion defect were not different by model (32% ± 10% of LV for the canine model and 31% ± 9% of LV for the porcine model). Risk area did not differ significantly when the heart was tomographically imaged within the closed-chest cavity (postmortem in situ scan) or with the addition of cardiac motion (premortem in vivo scan), as shown in Table 1. Consequently, there was close agreement between the risk area measured ex situ and the tomographic in vivo measurement. This finding reduces the likelihood that partial volume effects from wall motion abnormalities were present to any significant degree. Infarct size was significantly different by model, however (Fig. 3). The mean infarct size in the dog model was <1% of LV, with four of six animals demonstrating no identifiable myocardial necrosis by postmortem TTC staining. Conversely, infarct size was appreciably greater in the porcine model (14% ± 8% of LV; $p < 0.002$ when compared to infarct size in the canine model), with all animals in this group demonstrating some degree of myocardial necrosis (1%–22% of LV).

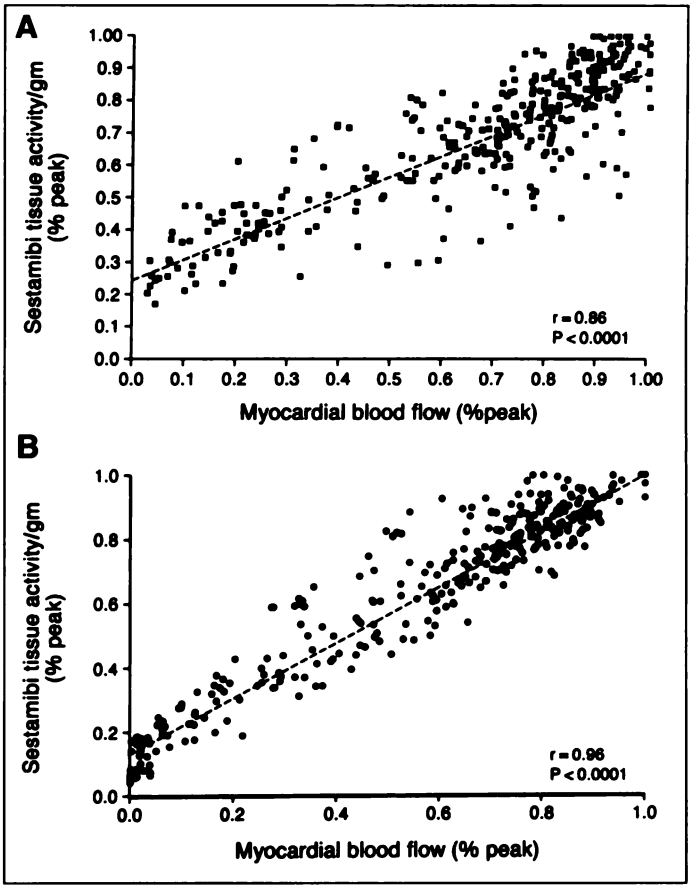

FIGURE 2. Linear correlation by segment between normalized myocardial blood flow and ^{99m}Tc-sestamibi activity for a canine model ($y = 0.66x + 0.25$) (A) and a porcine model ($y = 0.89x + 0.14$) (B). Note the small degree of overestimation of flow at low flow rates for both models.

Measures of Collateral Blood Flow

There was a significant inverse relationship between the degree of collateral flow as measured by radiolabeled microspheres and the risk area for all animals ($r = 0.53$, $p < 0.05$), but the confidence limits of this relationship were wide. The degree of collateral blood flow within the risk zone as measured by radiolabeled microspheres was significantly different between models, as shown in Figure 4: canine, 0.13 ± 0.09 $ml \cdot g^{-1} min^{-1}$, (range 0.02–0.27 $ml \cdot g^{-1} min^{-1}$); compared to

TABLE 1
Defect Extent by Technetium-99m-Sestamibi

Method	Extent of defect (%)			p value*
	All Animals	Canine	Porcine	
Ex situ slices	32 ± 9	32 ± 10	30 ± 9	NS
Tomographic imaging in situ				
Postmortem	30 ± 10	34 ± 9	28 ± 11	NS
Premortem	30 ± 10	31 ± 11	29 ± 10	NS
P value†	NS	NS	NS	

*Between canine and porcine models.
†Between imaging modalities (all animals and by model).
NS = not significant.

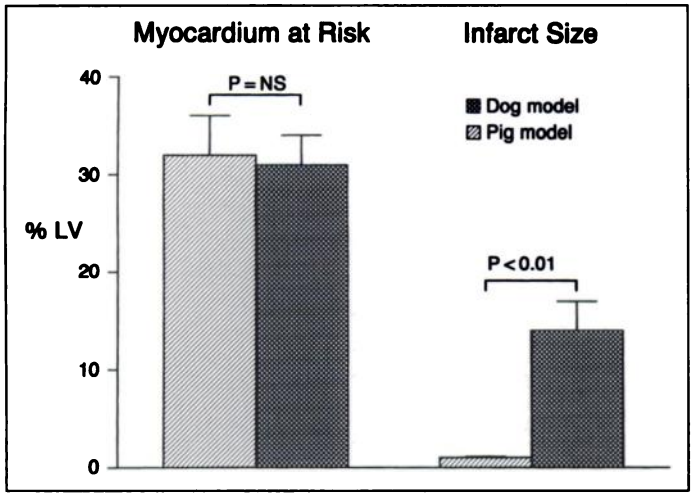

FIGURE 3. Mean and 95% confidence intervals of risk area (left) and infarct size (right) by model. The risk area was calculated from the ^{99m}Tc-sestamibi defect from the ex situ short-axis slices. Infarct size was determined by postmortem TTC staining.

porcine, 0.03 ± 0.05 $ml \cdot g^{-1} min^{-1}$ (range 0.005–0.14 $ml \cdot g^{-1} min^{-1}$) ($p < 0.05$; compared to central ischemic blood flow values). This difference remained significant whether a central ischemic value or a minimal value was compared. The severity of the perfusion defect (nadir) paralleled this pattern. Defect severity was more than 3-fold greater in the porcine model when the ex situ slices were compared (canine model, 0.23 ± 0.08; compared to porcine model, 0.07 ± 0.06; $p = 0.001$). This difference remained significant, although with less contrast, when tomographic imaging in vivo using the nadir ratio was analyzed (canine, 0.22 ± 0.10; compared to porcine, 0.11 ± 0.05; $p = 0.01$) (Fig. 4). Consequently, collateral blood flow was significantly different between the models, and ^{99m}Tc-sestamibi uptake within the risk zone demonstrated a similar pattern of difference whether imaged ex situ or tomographically in vivo.

Noninvasive Estimation of Collateral Flow

The primary analysis of this study was to determine the accuracy of tomographic imaging with ^{99m}Tc-sestamibi in measuring collateral blood flow, and the results are shown in Figure 5. The nadir of the perfusion defect was compared to absolute coronary blood flow, which was measured as either an average of three segments in the center of the risk zone (central ischemic flow) or with the minimal flow value by segment

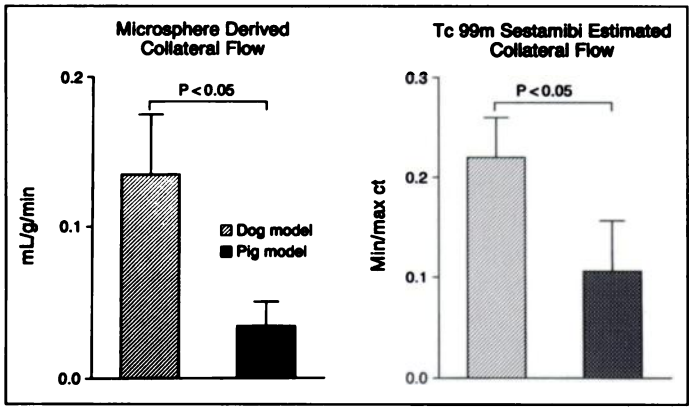

FIGURE 4. Mean and 95% confidence intervals of collateral flow measures by model. Microsphere-derived collateral flow (left) was significantly greater in the canine model. The tomographic radionuclide assessment of collateral flow (right) followed a similar pattern, showing significantly more residual ^{99m}Tc-sestamibi activity in the canine model.

within the risk zone (minimal blood flow). This imaging protocol for tomographic estimation of collateral flow replicates the clinical methodology in acute infarction treated with reperfusion therapy. The correlation was highly significant with both methods of microsphere derived measures of collateral blood flow, but the correlation was strongest with minimal blood flow values ($r = 0.90$), with a s.e. of the nadir value of 0.04. The correlation with normalized blood flow values (as a percentage of the peak blood flow value) was equally strong. Note that the intercept for each graph does not go through zero, suggesting a systematic overestimation of flow by ^{99m}Tc-sestamibi tomographic imaging, similar to the overestimation found at the tissue level. The relationship is linear, however. Consequently, an estimate of blood flow can be made for a tomographic nadir value. The s.e. of the estimate (4%–6%) suggests that such noninvasive estimates based on this linear relationship will reasonably reflect the degree of actual residual flow.

There was also a linear relationship between the nadir value from the sestamibi image (tomographic, in vivo) and infarct size by TTC staining (Fig. 6). Note that all animals with a nadir value of ≤0.10 (10% of maximal counts) had infarcts involving >5% of the LV. An example of a single-slice analysis from one of the pigs studied with very little collateral blood flow is shown in Figure 7.

DISCUSSION

The outcome of acute myocardial infarction has been shown in animal models to be primarily determined by the extent of the area at risk, the duration of coronary occlusion and any collateral flow present to sustain the jeopardized myocardium for the duration of occlusion (*1,2*). Sestamibi tomographic imaging in acute myocardial infarction has been shown to provide accurate measures of myocardium at risk and infarct size (*13–16*). Because the duration of coronary occlusion can be estimated from patient symptomatology, a comprehensive noninvasive analysis is potentially available using a single technique if residual blood flow to the jeopardized region can be measured. The results of this study, which replicate the clinical scenario of acute myocardial infarction, suggest that a reasonable estimate of the degree of collateral blood flow within the jeopardized zone can be obtained from tomographic imaging with an acute injection of ^{99m}Tc-sestamibi. Two models were chosen to provide a spectrum of collateral flow during occlusion: dogs, which usually have high native collateral flow; and pigs, which usually have scant native collaterals.

The correlation of ^{99m}Tc-sestamibi defect severity, determined by tomographic imaging, with actual collateral blood flow is possible due to the high correlation of these variables at the tissue level, despite restoration of reperfusion flow. In agreement with multiple prior reports, tissue sestamibi activity was linearly related to myocardial blood flow in normally perfused and ischemic myocardium when injected during occlusion but analyzed after reperfusion, but with some overestimation at low flow rates (*13,17,18*). The median correlation coefficients for both models, despite 1.5 hr–2.0 hr of reperfusion flow, were $r = 0.94$ and $r = 0.98$ for dogs and pigs, respectively. The close agreement seen at the tissue level between these two measurements was maintained when sestamibi activity was assessed with tomographic imaging, but with a consistent small degree of overestimation for both methods.

The results of this study are in agreement with those of Li et al. (*17*), who demonstrated a close association between coronary blood flow and tissue sestamibi activity with tomographic ^{99m}Tc-sestamibi imaging in an open-chest canine model using 6 min of occlusion. However, the short duration of occlusion used

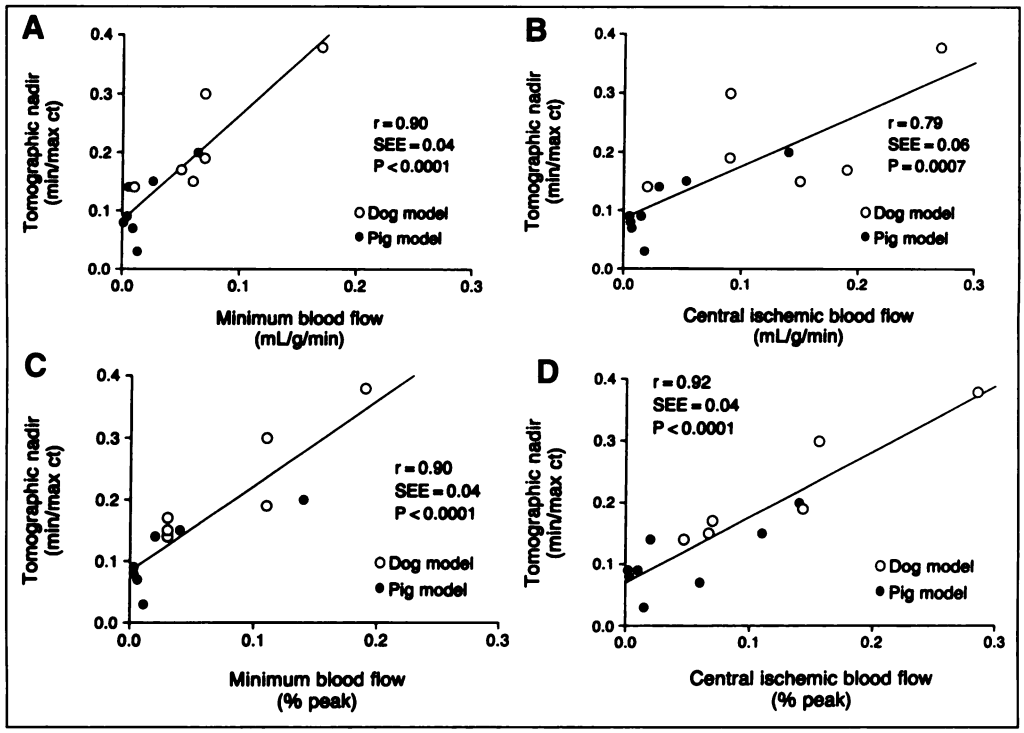

FIGURE 5. Correlation of the nadir from the tomographic ^{99m}Tc-sestamibi images with microsphere-derived blood flow measures. The primary analysis is shown in A and B, in which the comparison is to absolute blood flow values, either as a single minimal value within the risk zone (A) or as an average of three segments within the center of the risk zone (B). A secondary comparison of these methods of assessing collateral flow with microsphere flow normalized to peak flow within the LV (C,D). The linear regression equations for the figures are as follows. (A) y = 1.8x + 0.08. (B) y = 0.9x + 0.09. (C) y = 1.4x + 0.08 (D) y = 1.1x + 0.07.

by their model was not specifically designed to assess collateral flow. Technetium-99m-sestamibi was injected after only 1 min of coronary occlusion. Collaterals may not be fully recruitable during this short time period. We also felt that it was important to use a closed-chest model and variable models of collateral flow to more closely replicate the clinical scenario.

The extent of subsequent infarction was linearly related to the tomographic sestamibi defect nadir. However, this should be interpreted cautiously because the effect of collateral flow on infarct size is strongly influenced by the duration of coronary occlusion (*19*), which was kept constant in this series of experiments. Longer durations of occlusion may produce a different correlation.

The correlation seen in this study (r = 0.90) using an intravenous injection of ^{99m}Tc-sestamibi and standard closed-chest clinical imaging with actual collateral blood flow ($ml \cdot g^{-1} min^{-1}$) is closer than that reported with contrast echocardiography. Cheirif et al. (*20*) found a correlation between the echo contrast time intensity area and relative microsphere measured collateral flow of r = 0.72 in an open-chest canine preparation, in which the chest was filled with saline and the transducer was placed on the epicardial surface to enhance the acoustic interface. Additionally, the contrast injection was through the aortic root rather than intravenous. It is important to note these differences in methodology when comparing the results of the two techniques. Although contrast echocardiography has been shown to be predictive of improvement in wall motion in patients in the weeks after myocardial infarction (*7*), how well this modality will assess collateral flow using an intravenous injection during clinical acute myocardial infarction is uncertain.

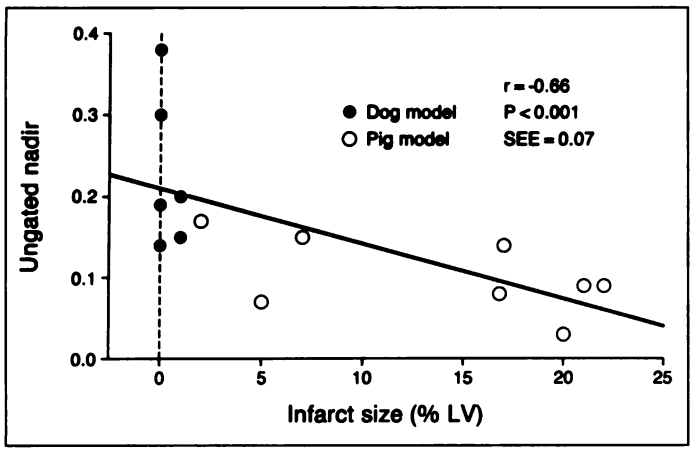

FIGURE 6. The correlation between the in vivo tomographic ungated nadir value from the ^{99m}Tc-sestamibi perfusion defect and subsequent infarct size by TTC staining postmortem. More severe defects were associated with a larger extent of infarction.

Although many collateral connections are below the resolution of cine angiographic imaging and are thus underestimated, the angiographic presence of collaterals before reperfusion therapy has been a strong predictor of outcome. Habib et al. (*3*), from the TIMI study group, found that, in patients who did not undergo reperfusion, infarct size was significantly smaller in patients with well-developed collaterals assessed during acute angiography than it was in patients without them. Left ventricular aneurysm formation has been found to be less prevalent in patients with well-developed collaterals after anterior infarction (*5*). Other investigators have found that angiographic collaterals are significantly associated with a reduction in infarct size, independent of myocardium at risk and time to reperfusion (*4,19,21*). However, not all institutions can perform coronary angiography during acute myocardial infarction, nor is it a practical strategy for patients receiving thrombolytic therapy. Consequently, a noninvasive method to assess residual flow to the jeopardized zone may be of value.

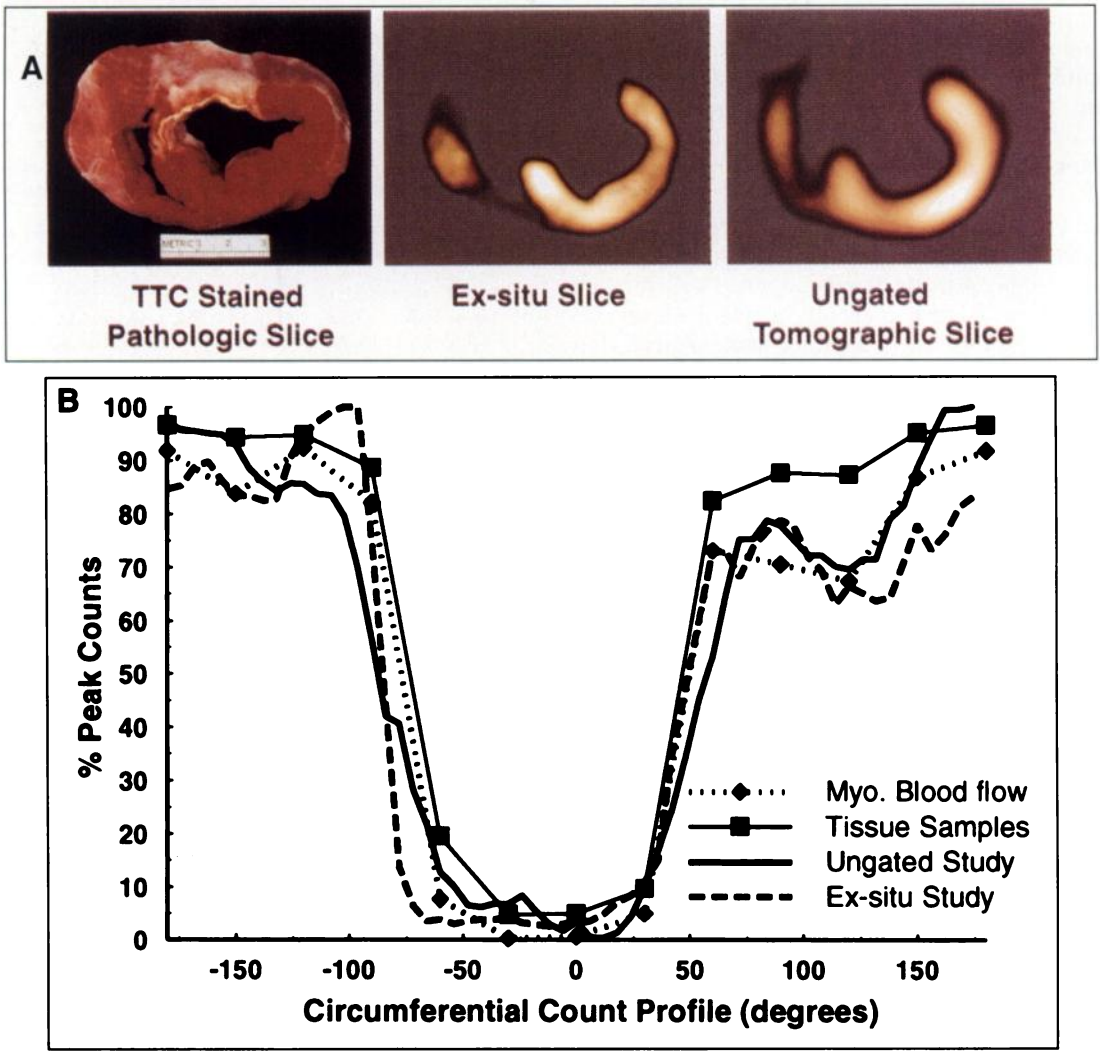

FIGURE 7. A short-axis slice at midventricle (third slice) of a pig who underwent balloon occlusion of the left anterior descending (A). Pathologic slice stained with TTC (left). The total amount of infarction for this particular slice was 23% of the slice (white region), and the total infarct size for the entire LV was 19% LV. Ex situ ^{99m}Tc-sestamibi acquisition (center). In vivo tomographic ^{99m}Tc-sestamibi scan (right). The perfusion images show a large anterior and septal defect at this level. The nadir value for the ex situ slice is 0.01 and the nadir of the in vivo tomographic slice is also 0.01. The total defect size for this animal was 41% of the LV by ex situ slices. Count profile curves from which the nadir values for the two perfusion images above were derived as well as tissue sestamibi activity and myocardial blood flow by radiolabeled microspheres (B).

Limitations and Technical Aspects

Tomographic sestamibi activity within the risk zone overestimated true myocardial blood flow in a small but consistent manner. This is likely due to several factors. In contrast to microspheres, which embolize and are entrapped within capillaries, the extraction of sestamibi can differ between ischemic and normal myocardium (*17,22*). Consequently, ischemic zones may have a higher ratio of sestamibi to microsphere activity than does normal myocardium, which appeared to be the case in this study, as evidenced by the tissue analysis. It is also conceivable that there is a small amount of redistribution of ^{99m}Tc-sestamibi into viable but previously ischemic tissue after reperfusion. Several studies have reported small degrees of redistribution of this agent in conjunction with stress studies (*23,24*). This is a possible confounder in this study, particularly in the dog model, in which the extent of necrosis was minimal, thus providing more hypoperfused but viable myocardium to be exposed to reperfusion flow. Prior animal studies examining this specific issue, however, have found it is not significantly important in models of reperfusion after prolonged occlusion (*25*). Additionally, photon scatter and tomographic reconstruction algorithms tend to "fill in" the nadir of a perfusion defect compared to in vitro counting (*26,27*). This physical property will impact on the tomographic measures by overestimating ^{99m}Tc-sestamibi activity within the defect. These factors combine to provide a small but consistent overestimation. However, the relationship between the nadir and myocardial blood flow was linear and quite close.

A correlate to the above discussion is the lack of inferior wall risk zones in the study group. Because of the deeper location within the thoracic cavity, inferior wall defects may be more influenced by scatter than anterior defects and can be expected to result in defects that appear less severe on this basis alone (*28*). Alternatively, such defects tend to be more attenuated (and therefore more severe) by overlying structures, so it is not clear what the overall effect on defect severity would be. The area at risk for inferior occlusion is markedly less than that for anterior occlusion and would have introduced considerable variation in the size of the area at risk (*29,30*). We have found in the clinical setting, however, that inferior perfusion defects by this methodology tend to be less severe than anterior defects (*4*).

Microspheres were injected into the LV of the pig model rather than into the left atrium. This was necessary due to the difficulty in performing trans-septal catheterization in a closed-chest pig. The slightly better correlation in the pig model between ^{99m}Tc-sestamibi activity injected intravenously com-

pared to the dog model argues against any significant streaming effect during microsphere injection into the LV cavity. In addition, a multibore pigtail catheter was used to facilitate adequate mixing. The values for blood flow within the risk zone during 40 min of occlusion are similar to those reported by other investigators in a 40-min open-chest canine occlusion model (0.12 $ml \cdot g^{-1} min^{-1}$) (*31*) and in a 45-min open-chest pig occlusion model (0.04 $ml \cdot g^{-1} min^{-1}$) (*32*). Consequently, completeness of occlusion by a percutaneous method and the mixing of the microspheres in the blood pool was likely present. Although great care was taken in manually slicing the heart into short-axis 1-cm slices, this was performed immediately after removing the heart from the chest, so there was some variation in slice thickness. However, in no case did such variability cause a second perfusion defect during the ex situ imaging.

CONCLUSION

Residual blood flow is an independent determinant of infarct size in the animal laboratory but has been difficult to quantify in the clinical setting of acute myocardial infarction. The ability of significant degrees of collateral flow to extend the time window for the benefit of reperfusion after coronary occlusion has been demonstrated in animal-based studies (*2,3*). Such studies have shown that a random over-representation of subjects with high collateral flow during coronary occlusion can provide erroneous conclusions as to the efficacy of a reperfusion strategy (*1*). This technique has previously been shown to be clinically feasible and to provide independent information on final infarct size in patients treated with reperfusion therapy (*4*). With a reliable method to assess collateral flow, it is conceivable that clinical decisions regarding the administration of reperfusion therapy for patients who present with acute myocardial infarction either late or with relative contraindications to such therapy can be facilitated. More relevant to the design of this study, an accurate measure to estimate collateral flow during coronary occlusion but acquired after the administration of reperfusion therapy can be incorporated into clinical trials along with myocardium at risk and time to reperfusion measures to compare the efficacy of therapeutic strategies for acute infarction (*4,33*). Prospective clinical trials are necessary to determine whether such measures can provide insight into the variability in outcome in acute myocardial infarction.

ACKNOWLEDGMENTS

This study was supported by a grant from the Mayo Foundation (Rochester, MN). We would like to acknowledge the assistance of Patricia Beighley, Wayne Blanchard, Steve Jorgensen, Michelle Rank, Ladonna Camrud, Sandy Hein and Jami Spitzer, without whose help this study would not have been possible.

REFERENCES

1. Reimer KA, Jennings RB, Cobb FR, et al. Animal models for protecting ischemic myocardium: results of the NHLBI cooperative study. Comparison of unconscious and conscious dog models. *Circ Res* 1985;56:651–665.
2. Murdock RH Jr, Chu A, Grubb M, Cobb FR. Effects of reestablishing blood flow on extent of myocardial infarction in conscious dogs. *Am J Physiol* 1985;249:783–791.
3. Habib GB, Heibig J, Forman SA, et al. Influence of coronary collateral vessels on myocardial infarct size in humans. Results of phase I thrombolysis in myocardial infarction trial. *Circulation* 1991;83:739–746.
4. Christian TF, Schwartz RS, Gibbons RJ. Determinants of infarct size in reperfusion therapy for acute myocardial infarction. *Circulation* 1992;86:81–90.
5. Saito Y, Yasuno M, Ishida M, et al. Importance of coronary collaterals for restoration of left ventricular function after intracoronary thrombolysis. *Am J Cardiol* 1985;55: 1259–1263.
6. Williams DO, Amsterdam EA, Miller RR, Mason DT. Functional significance of coronary collateral vessels in patients with acute myocardial infarction: relation to pump performance, cardiogenic shock and survival. *Am J Cardiol* 1976;37:345–351.
7. Sabia PJ, Powers ER, Rageosta M, Sarembock IJ, Burnell LR, Kaul SJ. An association between collateral blood flow and myocardial viability in patients with recent myocardial infarction. *N Engl J Med* 1992;327:1825–1831.
8. Gibbons RJ, Holmes DR, Reeder GS, Bailey KK, Hopfenspirger MR, Gersh BJ. Immediate angioplasty compared with the administration of a thrombolytic agent followed by conservative treatment for myocardial infarction. *N Engl J Med* 1993; 328:685–691.
9. O'Connor MK, Hammell TC, Gibbons RJ. In vitro validation of a simple tomographic technique for estimation of percent myocardium "at risk" following administration of Tc-99m isonitrile. *Eur J Nucl Med* 1990;17:69–76.
10. Christian TF, O'Connor MK, Glynn RB, Rogers PJ, Gibbons RJ. The influence of gating on measurements of myocardium at risk and infarct size during acute myocardial infarction by tomographic Tc-99m labeled sestamibi imaging. *J Nucl Cardiol* 1995;2:207–216.
11. Domenech RJ, Hoffman JIE, Noble MIM, Saunders KB, Henson JR, Subijanto S. Total and regional coronary blood flow measured by radioactive microsphere in conscious and anesthetized dogs. *Circ Res* 1969;25:581–596.
12. Buckberge GD, Luck JE, Payne DB, Hoffman JIE, Archie JP, Fixler DE. Some sources of error in measuring blood flow with radioactive microspheres. *J Appl Physiol* 1971;31:598–604.
13. Sinusas AJ, Trautman KA, Bergin JD, et al. Quantification of "area at risk" during coronary occlusion and degree of myocardial salvage after reperfusion with technetium-99m-methoxyisobutyl-isonitrile. *Circulation* 1990;82:1424–1437.
14. Verani MS, Jeroudi MO, Mahmarian JJ, et al. Quantification of myocardial infarction during coronary occlusion and myocardial salvage after reperfusion using cardiac imaging with technetium-99m-hexakis-2-methoxy-isobutyl isonitrile. *J Am Coll Cardiol* 1988;12:1573–1581.
15. Christian TF, Behrenbeck T, Pellikka, PA, Huber KC, Chesebro JH, Gibbons RJ. Mismatch of left ventricular function and infarct size demonstrated by technetium-99m-isonitrile imaging after reperfusion therapy for acute myocardial infarction: identification of myocardial stunning and hyperkinesia. *J Am Coll Cardiol* 1990;16:1632–1638.
16. Chareonthaitawee P, Christian TF, Hirose K, Gibbons RJ, Rumberger JA. The relationship of infarct size with the extent of left ventricular remodeling following myocardial infarction. *J Am Coll Cardiol* 1995;25:567–573.
17. Li QS, Frank TL, Franceschi D, Wagner HN, Becker LC. Technetium-99m methoxyisobutyl isonitrile (RP30) for quantification of myocardial ischemia and reperfusion in dogs. *J Nucl Med* 1988;29:1539–1548.
18. Okada RD, Glover D, Gaffney T, William S. Myocardial kinetics of technetium-99m-hexakis-2-methoxy-2-isonitrile. *Circulation* 1988;77:491–498.
19. Murdock RH Jr, Chu A, Grubb M, Cobb FR. Effects of reestablishing blood flow on extent of myocardial infarction in conscious dogs. *Am J Physiol* 1985;249:783–791.
20. Cheirif BJ, Warkiewicz-Judko JB, Hawkins HK, Bravenec JS, Quinones MA, Mickelson JK. Myocardial contrast echocardiography; relation of collateral perfusion to extent of injury and severity of contractile dysfunction in a canine model of coronary thrombosis and reperfusion. *J Am Coll Cardiol* 1995;26:537–546.
21. Rogers WJ, Hood WP Jr, Mantle JA, et al. Return of left ventricular function after reperfusion in patients with myocardial infarction: importance of subtotal stenosis or intact collaterals. *Circulation* 1984;69:338–349.
22. Meerdink DJ, Leppo JA. Comparison of hypoxia and oubain effects on the myocardial uptake kinetics of technetium-99m hexakis 2-methoxy isobutyl isonitrile and thallium-201. *J Nucl Med* 1989;30:1500–1506.
23. Taillefer R, Primeau M, Costi P, Lambert R, Leveille J, Latour Y. Technetium-99m-sestamibi myocardial perfusion imaging in detection of coronary artery disease: comparison between initial (1-hour) and delayed (3-hour) postexercise images. *J Nucl Med* 1991;32:1961–1965.
24. Sinusas AJ, Bergin JD, Edwards EC, et al. Redistribution of Tc-99m sestamibi and thallium-201 in the presence of a severe coronary artery stenosis. *Circulation* 1994;89:2332–2341.
25. DeCoster PM, Wijns W, Cauwe F, Robert A, Beckers C, Melin JA. Area at risk determination by technetium-99m-hexakis-2-methoxy-isobutyl-isonitrile in experimental reperfused myocardial infarction. *Circulation* 1990;82:2151–2162.
26. Caldwell JH, Williams DL, Hamilton GW, et al. Regional distribution of myocardial blood flow measured by single photon emission tomography: comparison with in-vitro counting. *J Nucl Med* 1984;25:788–791.
27. Chang W, Henkin RE, Buddemeyer E. The sources of overestimation in the quantification by SPECT of uptakes in a myocardial phantom: concise communication. *J Nucl Med* 1994;74:II-297.
28. O'Connor MK, Caiati C, Christian TF, Ribbons RJ. Effects of scatter correction on the measurement of infarct size from SPECT cardiac phantom studies. *J Nucl Med* 1995;36:2080–2086.
29. Christian TF, Gibbons RJ, Gersh BJ. Effect of infarct location on myocardial salvage assessed by technetium-99m-isonitrile. *J Am Coll Cardiol* 1991;17:1303–1308.
30. Feiring AJ, Johnson MR, Kioschos JM, et al. The importance of the determination of the myocardial area at risk in the evaluation of the outcome of acute myocardial infarction in patients. *Circulation* 1987;75:980–987.
31. Reimer KA, Jennings RB. The wavefront phenomenon of myocardial ischemic cell death. II. Transmural progression of necrosis within the framework of ischemic bed size (myocardium at risk) and collateral flow. *Lab Invest* 1979;40:633–644.
32. Amsterdam EA, Pan HL, Rendig SV, Symons JD, Fletcher MP, Longhurst JC. Limitation of myocardial infarct size in pigs with a dual lipoxygenase-cyclooxygenase blocking agent by inhibition of neutrophil activity without reduction of neutrophil migration. *J Am Coll Cardiol* 1993;22:1738–1744.
33. Christian TF, Gibbons RJ, Clements IP, Berger PB, Selvester RH, Wagner GS. Prediction of myocardium at risk and collateral flow in acute myocardial infarction using electrocardiographic indices with comparison to radionuclide and angiographic measures. *J Am Coll Cardiol* 1995;26:388–393.